SUPPLEMENTAL RESEARCH DESIGN AND METHODS:

Glucose and Insulin Tolerance Assessment: Glucose and insulin tolerance tests were performed 6 hr after food withdrawal using glucose and insulin doses of 2 g/kg and 0.3 U/kg, IP, respectively. In *db/db* mice, animals were fasted overnight and glucose and insulin doses were 1 g/kg and 0.7 U/kg, IP, respectively. Blood glucose measurements were performed via tail bleed with the Accu Check Advantage system (Roche®). In another experiment, DIO or *db/db* mice were fasted for 6 hr or overnight, respectively, and injected IP with insulin doses of 0.3 U/kg or 0.7 U/kg, respectively. At 30 min post-insulin injection, animals were sacrificed and gastrocnemius muscle was isolated and harvested in the appropriate conditions for immunoblot assessment of proteins involved in the insulin signaling pathway (see below).

Meal Tolerance Testing: Meal tolerance tests were performed in animals fasted overnight via supplementation of a 5 g pellet of standard laboratory animal chow. Blood glucose measurements were performed via tail bleed with the Accu Check Advantage system (Roche®). Plasma was also collected at the 0, 30 and 60 min time points in EGTA coated tubes (Sarstedt).

Plasma Insulin Levels: Plasma insulin concentrations were determined via use of a commercially available enzyme-linked immunosorbent assay kit (Alpco Diagnostics). 5 µL of each sample was added to each well with 75 µL of a provided enzyme conjugate, and the 96 well plate was then incubated for 2 hr at room temperature on an orbital microplate shaker at ~700-900 RPM. After incubation, the plate was washed 6x with a provided working strength wash buffer, and then 100 µL of a provided substrate was added to each well to start the reaction, which was terminated after 30 min via addition of 100 µL of stop solution. Any air bubbles were removed and plasma insulin levels "ng/mL" were determined via reading the absorbance of the plate at a wavelength of 450 nm.

Intramyocellular Lipid Metabolite Assessment: Extraction of long chain acyl CoA esters via high performance liquid chromatography (HPLC) was performed as previously described (1). Triacylglycerols were extracted with a 2:1 chloroform-methanol solution and quantified with an enzymatic assay kit (Wako Pure Chemical Industries) as previously described (2). Ceramides were extracted as previously described (3). In brief, tissue was extracted with 1 mL of a 1:1:1 chloroform-methanol-1 *N* HCl in the presence of 0.3 mL saline solution. The resulting organic phase was separated and dried under N_2. 0.5 mL of 1 M KOH in 90% (v/v) methanol is added and samples are heated at 90^{o}C for 1 hr to deacylate ceramide into sphingosine. Samples are then extracted with 1 M HCl in methanol, chloroform, and 1 M aqueous NaCl. The resulting organic phase is dried under N_2, redissolved in methanol, and derivatized to *o*-Phthalaldehyde to generate a fluorescent compound that is separated by HPLC and quantified by fluorescence spectrometry. Diacylglycerols were extracted as previously described (4). In brief, ~5 mg of gastrocnemius tissue was homogenized in 0.8 ml of 1 mM NaCl. The homogenate is then transferred over to a 13 x 100 mm test tube and extracted with 3.0 ml of 1:2 chloroform-methanol and mixed. 1 ml of 1 mM NaCl and chloroform is then added to break phases and the resulting sample is centrifuged briefly at 5,000 x*g* to separate the organic and aqueous phases. The chloroform phase is then collected and evaporated under N_2 gas. The lipids are then solubilized with a 7.5% octyl-β-D-glucoside/5mM cardiolipin/1mM DETAPAC solution and incubated at room temperature for 5 – 15 min. The sample is then brought to 100 µl volume

with 50 µl of 2x reaction buffer, 20 µl 10 mM DTT and 10 µl DAG kinase (0.5 mg/ml). The reaction is initiated by the addition of 10 µl of 10 mM ATP (mixed with [γ-^{32}P]ATP) and incubated for 30 min at 25^{o}C. 3 mL chloroform/methanol (1:2) and 0.7 mL 1% $HClO_4$ is then added to each tube and mixed before the addition of 1 mL chloroform and 1 mL 1% $HClO_4$. The phases are then separated via centrifugation at 2,000 x*g* at 4^{o}C for 5 min. The aqueous phase is discarded and the chloroform phase washed twice with 2 ml of 1% $HClO_4$. The sample is then evaporated under N_2 gas and dissolved in 100 µl of 5% methanol in chloroform. 20 µl of each sample is spotted onto a thin layer chromatography (TLC) plate and activated by acetone (develop with choloroform/methanol/acetic acid (65:15:5)). After TLC plate has ran, the plate is exposed to X-ray film and developed for ~48 hrs. Finally, the silicon is scraped off the plate into 5 ml scintillation vials with 4 ml of scintillation solution (Ecolite, ICN) and ^{32}P counted in a liquid scintillation counter.

Metabolic Profiling: Metabolic profiling of tissues (i.e. gastrocnemius) involved quantitation by gas chromatography – mass spectrometry (GC/MS) based on dilution of stable-isotope-labeled internal standards (D3-C14:0, D3-C16:0, D3-C18:0, and 13C1-C18:1; CDN isotopes, Pointe-Claire, Quebec, and Isotec, St. Louis, MO), using a Trace Ultra GC coupled to a Trace DSQ MS (Thermo Fisher Scientific, Austin, TX). Acylcarnitine measurements were made using flow injection tandem MS of samples (~20 mg of tissue) homogenized in 20-fold volume of deionized H_2O as previously described (5). Data were acquired using a Micromass Quattro MicroTM system equipped with a model 2777 autosampler, a model 1525 high performance liquid chromatography (HPLC) solvent delivery system and a data system controlled by MassLynx 4.0 operating system (Waters, Millford, MA). The remaining lysate from the acylcarnitine preparation was subjected to 1 freeze-fracture cycle in liquid N_2, immediately thawed at room temperature and sonicated with a small pencil-tip probe at ~3 watts for 5 sec. The sonicated lysate was then centrifuged at 14,000 x *g* for 15 min at 4^{o}C, and organic acids were quantified from the resulting supernatant using methods previously described (6) employing Trace Ultra GC coupled to Trace DSQ MS operating under Excalibur 1.4 (Thermo Fisher Scientific, Austin, TX).

Exercise Capacity Testing: Exercise capacity was performed by running animals on a calibrated, motor-driven treadmill (Columbus Instruments) at a speed of 3 m/min for 1 min, followed by increasing speeds of 4 m/min for 1 min, 5 m/min for 1 min, 6 m/min for 3 min, 8 m/min for 14 min, 9 m/min for 10 min, 10 m/min for 7 min, 12 m/min for 7 min, and 14 m/min until exhaustion. The first 6 min were used as an acclimatization period for the animals to become familiar with the treadmill and not used for data collection. Exhaustion was determined as the animal spending >10 consecutive seconds on the shock grid, or the animal running off the shock grid and immediately falling back onto the shock grid 3 consecutive times.

Whole body In Vivo Metabolic Assessment: In vivo metabolic assessment via indirect calorimetry was performed using the Oxymax CLAMS (Columbus Instruments). Animals were initially acclimatized in the system for a 24 hr period, the subsequent 24 hr period was utilized for data collection.

Citrate Synthase Activity Assay: Frozen gastrocnemius tissue (5 – 10 mg) or C2C12 myotubes were homogenized in buffer containing 50 mM Tris HCl (pH 8 at 4^{o}C), 1 mM EDTA, 10%

glycerol (w/v), 0.02% Brij-35 (w/v), 1 mM dithiothreitol (DTT), protease and phosphatase inhibitors (Sigma). After homogenization for 30 sec, the homogenate was left on ice for 10 min before centrifugation at 10,000 x *g* for 20 min. The resulting supernatant was brought to a final dilution of 1/50, and 2 µL of each sample was pipetted into a 96 well plate. Each well was brought to a final volume of 190 µL with 184 µL of assay buffer (100 mM Tris HCl, 1 mM EDTA, 1 mM $MgCl_2$), 2 µL of 5,5'-dithiobis-(2-nitrobenzic acid) (DNTB), and 2 µL of 30 mM acetyl CoA. The reaction was then initiated by the addition of 10 µL of 10 mM oxaloacetic acid and the reaction mixture has its absorbance followed at a 412 nM wavelength for a 2 min duration (readings taken in 30 sec intervals) with a spectrophotometer kinetic plate reader. The 96 well plate was read at a 412 nM wavelength for a 2 min duration as well before the addition of oxaloacetic acid in order to obtain a baseline reading. The final reading was multiplied by 60 to obtain a rate per min, and citrate synthase (CS) activity in "µmol/min/g wet weight" was calculated with the following equation;

($\Delta Absorbance_{412}$/min x 0.2 mL (volume of reaction)) / (13.6 (ε for DNTB) x 0.552 (pathlength for 96 well plate) x 0.02 (mg of tissue in reaction))

β-Hydroxyacyl CoA Dehydrogenase Activity Assay: Frozen gastrocnemius tissue (5 – 10 mg) was homogenized in buffer containing 50 mM Tris HCl (pH 8 at 4°C), 1 mM EDTA, 10% glycerol (w/v), 0.02% Brij-35 (w/v), 1 mM DTT, protease and phosphatase inhibitors (Sigma). After homogenization for 30 sec, the homogenate was left on ice for 10 min before centrifugation at 10,000 x *g* for 20 min. The resulting supernatant was brought to a final dilution of 1/20, and 10 µL of each sample was pipetted into a 96 well plate. Each well was brought to a final volume of 190 µL with 160 µL of 50 mM imidazole (pH 7.4) and 20 µL of 1.5 mM NADH. The reaction was then initiated by the addition of 10 µL of 2 mM acetoacetyl CoA and the reaction mixture has its absorbance followed at a 340 nM wavelength for a 5 min duration (readings taken in 30 sec intervals) with a spectrophotometer kinetic plate reader. The 96 well plate was read at a 340 nM wavelength for a 5 min duration as well before the addition of acetoacetyl CoA in order to obtain a baseline reading. The final reading was multiplied by 60 to obtain a rate per min, and β-hydroxyacyl CoA Dehydrogenase (βHAD) activity in "µmol/min/g wet weight" was calculated with the following equation;

($\Delta Absorbance_{340}$/min x 0.2 mL (volume of reaction)) / (6.22 (ε for NADH disappearance) x 0.552 (pathlength for 96 well plate) x 0.4 (mg of tissue in reaction))

Cell Culture: C2C12 skeletal muscle myotubes (ATCC, Rockville, MD, USA) were grown as myoblasts to confluency in 60 mm diameter cell culture dishes in DMEM containing 10% (v/v) fetal bovine serum, 1% (v/v) PenStrep and 0.25 mM L-carnitine. Dishes were incubated in a water-jacketed CO_2 incubator maintained at 37°C with 95% O_2 and 5% CO_2 (v/v/v). Replenishment with fresh media occurred every 48 h. On reaching approximately 90% confluency, myoblasts were allowed to differentiate into myotubes in DMEM containing 2% (v/v) horse serum, 1% (w/v) penstrep, and 0.25 mm l-carnitine. Passages 10 – 15 were used for experiments described in this study.

Immunoblot Analysis: Frozen gastrocnemius tissue (25-30 mg) was homogenized in buffer containing 50 mM Tris HCl (pH 8 at 4°C), 1 mM EDTA, 10% glycerol (wt/vol), 0.02% Brij-35

(wt/vol), 1 mM dithiothreitol, protease and phosphatase inhibitors (Sigma). After homogenization for 30 s, the homogenate was left on ice for 10 min before centrifugation at 10,000 x *g* for 20 min. The resulting supernatant was processed for immunoblotting. Protein concentration of homogenates was determined via Bradford protein assay kit (Bio-Rad). Samples (20 μg protein each) were resolved via 8% sodium dodecyl sulfate polyacrylamide gel electrophoresis (SDS-PAGE) and transferred onto a 0.45 μm nitrocellulose membrane. Membranes were blocked with 10% fat free milk for 2 hours and probed with either anti-Akt (Cell Signaling Technologies, 1/1000 dilution), anti-phosphoSerine-473 Akt (Cell Signaling Technologies, 1/500 dilution), anti-GSK3β (Cell Signaling Technologies, 1/1000 dilution), anti-phosphoSerine-9 GSK3β (Cell Signaling Technologies, 1/500 dilution), anti-p38 MAPK (Cell Signaling Technologies, 1/1000 dilution), anti-phosphoThreonine-180 p38 MAPK (Cell Signaling Technologies, 1/500 dilution), anti-JNK (Cell Signaling Technologies, 1/1000 dilution), anti-phosphoThreonine-180 JNK (Cell Signaling Technologies, 1/500 dilution), anti-PGC1α (Santa Cruz Biotechnology, 1/200 dilution), or anti-actin (Santa Cruz Biotechnology, 1/200 dilution, 1/1000 dilution) antibodies in 5% fatty acid free BSA. Membranes were then washed with 1x phosphate buffered saline and subsequently probed with goat anti-rabbit (Santa Cruz Buitechnology, 1/2000 dilution) secondary antibody in 1% fat-free milk. Immunoblots were visualized with the enhanced chemiluminescence Western blot detection kit (Perkin Elmer) and quantified with Quantity One (4.4.0) Software (Biorad Laboratories).

Statistical Analysis: All values are presented as mean ± SE (*n* observations). The significance of differences was determined by the use of an unpaired, 2-tailed Student's *t*-test, two-way analysis of variance (ANOVA), or a one-way ANOVA followed by a Bonferroni post-hoc analysis where appropriate. Differences were considered significant when $P < 0.05$.

Supplemental Reference List:

1. Gao S, Kinzig KP, Aja S, Scott KA, Keung W, Kelly S, Strynadka K, Chohnan S, Smith WW, Tamashiro KL, Ladenheim EE, Ronnett GV, Tu Y, Birnbaum MJ, Lopaschuk GD, Moran TH: Leptin activates hypothalamic acetyl-CoA carboxylase to inhibit food intake. *Proc Natl Acad Sci U S A* 104:17358-17363, 2007

2. Atkinson LL, Kozak R, Kelly SE, Onay Besikci A, Russell JC, Lopaschuk GD: Potential mechanisms and consequences of cardiac triacylglycerol accumulation in insulin-resistant rats. *Am J Physiol Endocrinol Metab* 284:E923-930, 2003

3. Bose R, Kolesnick R: Measurement of ceramide levels by the diacylglycerol kinase reaction and by high-performance liquid chromatography-fluorescence spectrometry. *Methods Enzymol* 322:373-378, 2000

4. Preiss J, Loomis CR, Bishop WR, Stein R, Niedel JE, Bell RM: Quantitative measurement of sn-1,2-diacylglycerols present in platelets, hepatocytes, and ras- and sis-transformed normal rat kidney cells. *J Biol Chem* 261:8597-8600, 1986

5. An J, Muoio DM, Shiota M, Fujimoto Y, Cline GW, Shulman GI, Koves TR, Stevens R, Millington D, Newgard CB: Hepatic expression of malonyl-CoA decarboxylase reverses muscle, liver and whole-animal insulin resistance. *Nat Med* 10:268-274, 2004

6. Jensen MV, Joseph JW, Ilkayeva O, Burgess S, Lu D, Ronnebaum SM, Odegaard M, Becker TC, Sherry AD, Newgard CB: Compensatory responses to pyruvate carboxylase suppression in

islet beta-cells. Preservation of glucose-stimulated insulin secretion. *J Biol Chem* 281:22342-22351, 2006

Figure 1: The effect of chronic high fat feeding on body weight and insulin sensitivity
A: Body weight in mice following 12 weeks of high fat feeding. *B:* Development of glucose intolerance, and *C:* insulin resistance following 11 weeks of high fat feeding. *D:* Respective % change in blood glucose levels during the insulin tolerance test. Values represent mean ± SE (n = 15). Differences were determined using a two-way ANOVA followed by a Bonferroni post-hoc analysis. **P*<0.05, significantly different from the low fat diet mice.

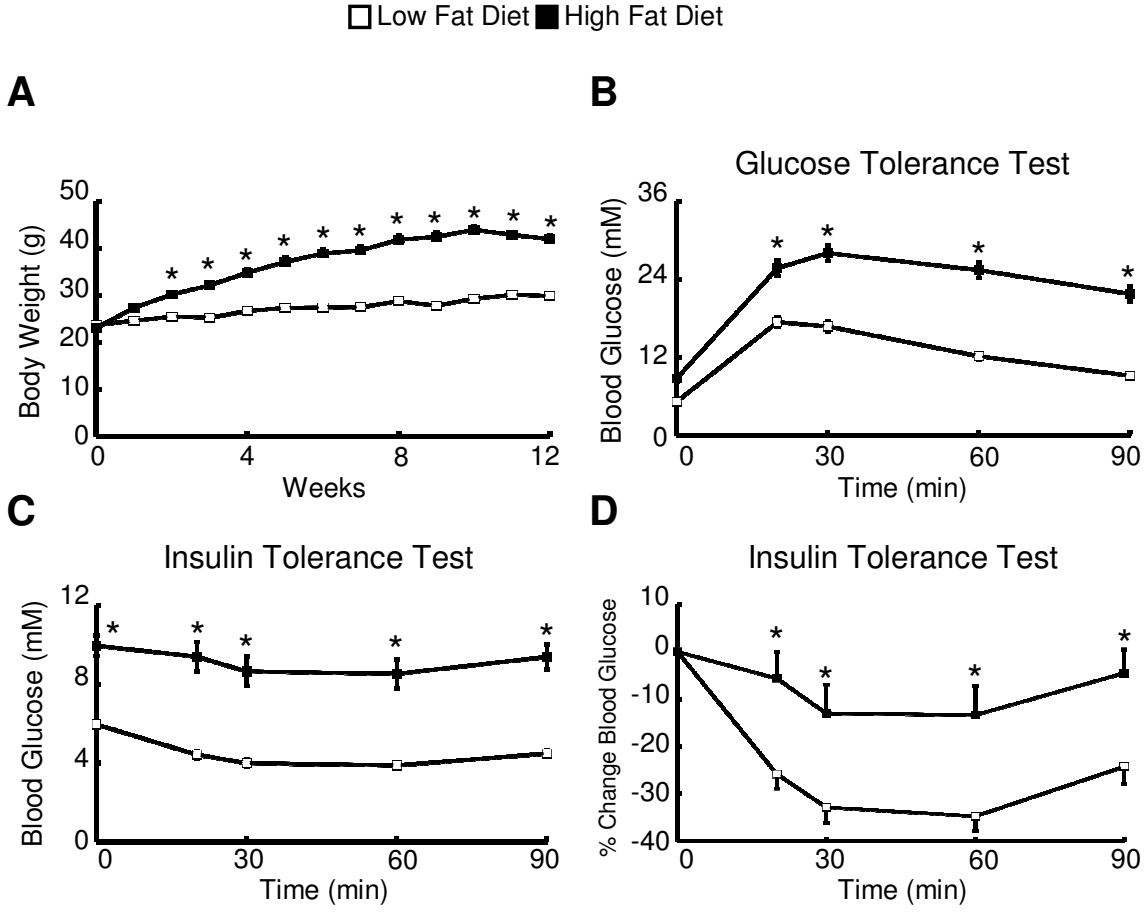

Figure 2: High fat diet-induced insulin resistance is associated with a dramatic shift in substrate preference and an impairment of whole body oxygen consumption.
Following 11 weeks of high fat feeding, *A:* 24 hr respiratory exchange ratio (RER), *B:* dark and light cycle RER, *C:* 24 hr whole body oxygen consumption, and *D:* dark and light cycle whole body oxygen consumption were assessed. Values represent mean ± SE (n = 6). Differences were determined using a two-way ANOVA followed by a Bonferroni post-hoc analysis. **P*<0.05, significantly different from the low fat diet counterpart. †*P*<0.05, significantly different from the dark cycle counterpart.

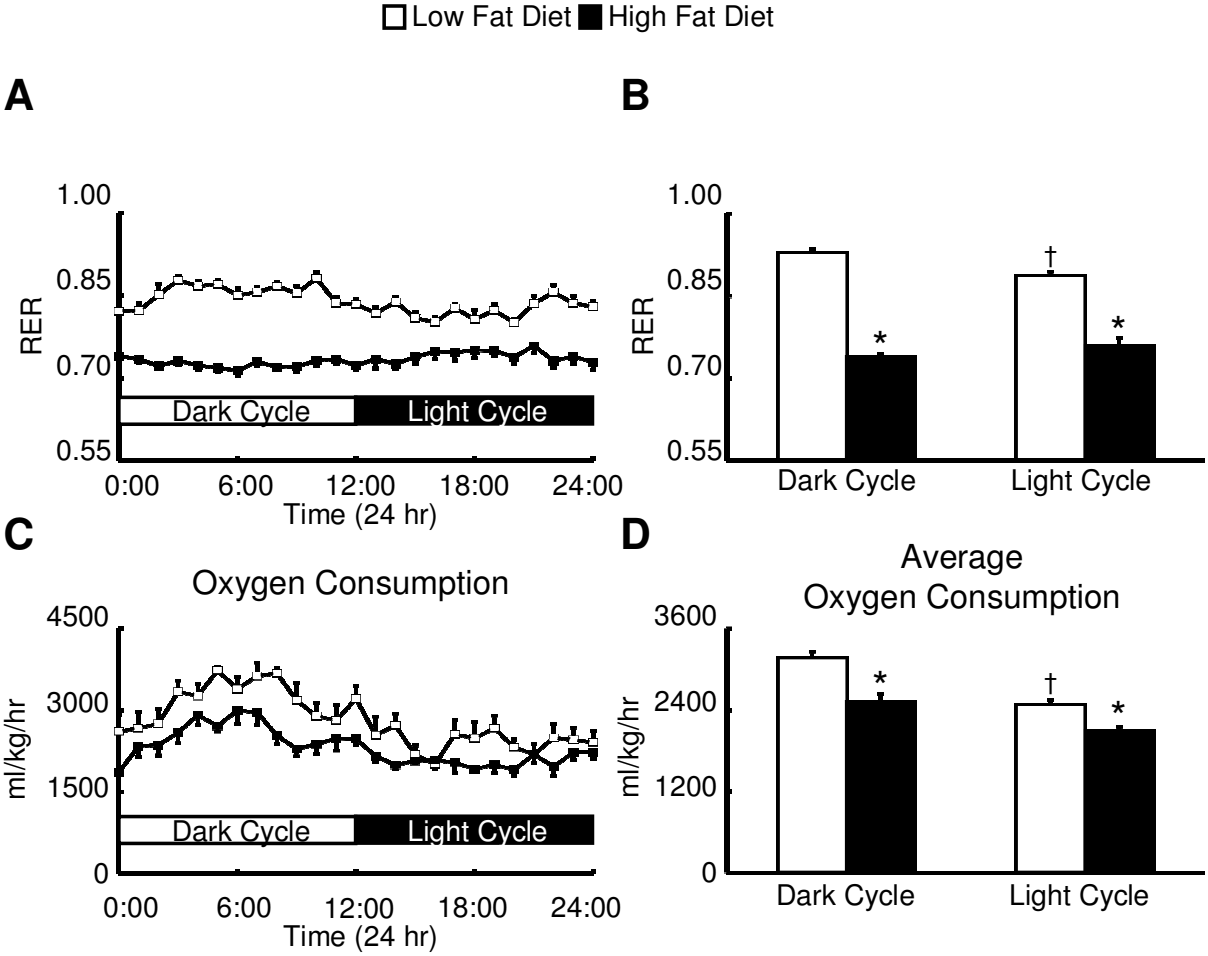

Figure 3: L-cycloserine treatment improves control of plasma insulin levels in JCR:LA cp obese rats following a meal tolerance test.
Plasma insulin levels were determined at the 0, 30, and 60 min time points post-chow pellet consumption in heterozygous lean, JCR:LA cp obese, and JCR:LA cp obese L-cycloserine treated rats following a meal tolerance test. Values represent mean ± SE (n = 4-5). Differences were determined using a one-way ANOVA followed by a Bonferroni post-hoc analysis. **P*<0.05, significantly different from heterozygous lean rats. †*P*<0.05, significantly different from JCR:LA cp obese rats.

Figure 4: L-cycloserine treatment reverses high-fat diet induced insulin resistance.
A: Blood glucose levels during a glucose tolerance test (GTT) in obese-insulin resistant mice treated with either vehicle control or L-cycloserine. *B:* Area under the curve (AUC) during the GTT. *C:* Blood glucose levels during an insulin tolerance test (ITT) in obese-insulin resistant mice treated with either vehicle control or L-cycloserine. *D:* % Change in blood glucose levels during the ITT. Values represent mean ± SE (n = 5-7). Differences were determined using either a 2-tailed Student's *t*-test or a two-way ANOVA followed by a Bonferroni post-hoc analysis. **P*<0.05, significantly different from the high fat diet control mice.

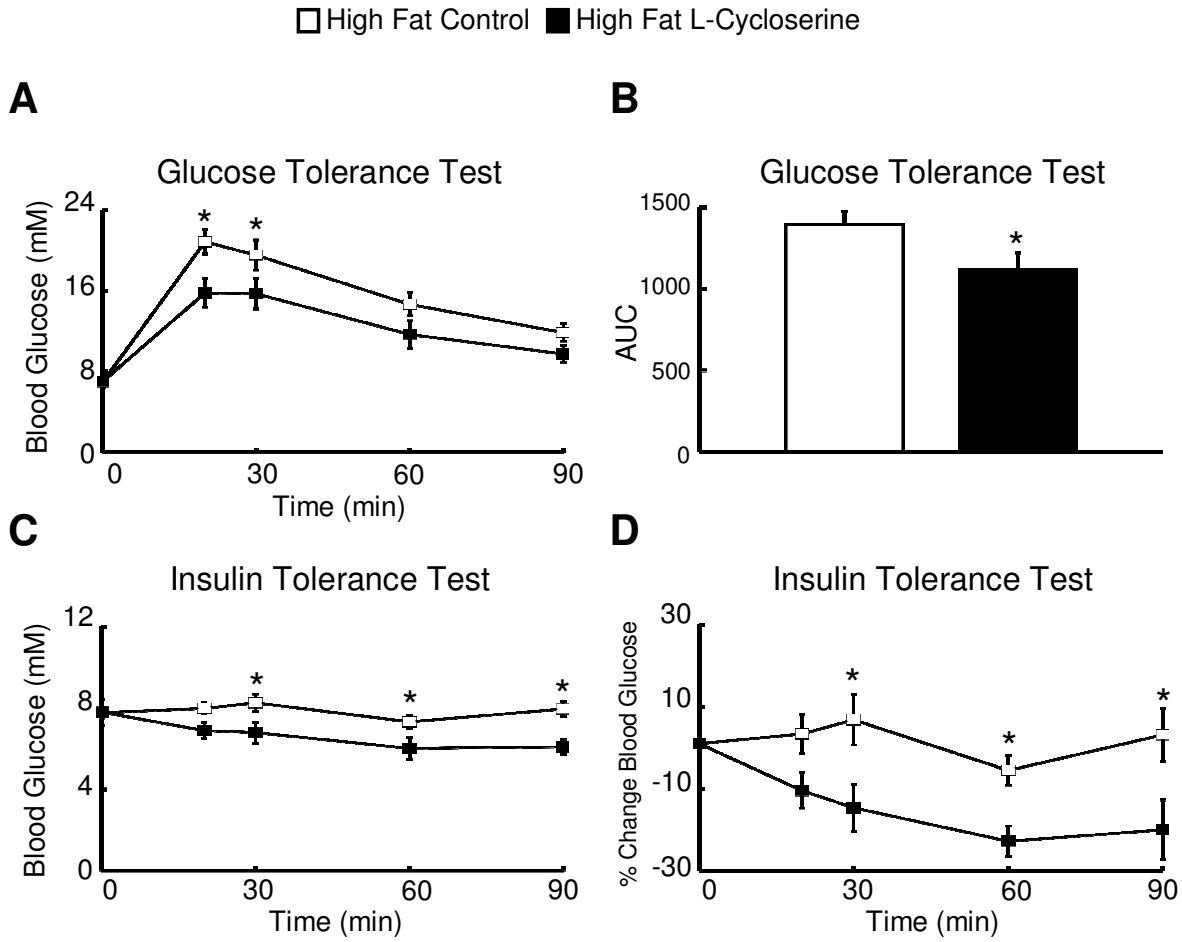

Figure 5: Heat production and activity in lean and obese mice.
A: Dark cycle and *B:* Light cycle heat production in low fat diet and obese-insulin resistant mice treated with either vehicle control or myriocin. *C:* Dark cycle, *D:* Light cycle and *E:* 24 hr ambulatory activity in low fat diet and obese-insulin resistant mice treated with either vehicle control or myriocin. Values represent mean ± SE (n = 8-12). Differences were determined using a two-way ANOVA followed by Bonferroni post-hoc analysis. **P*<0.05, significantly different from the low fat diet counterpart.

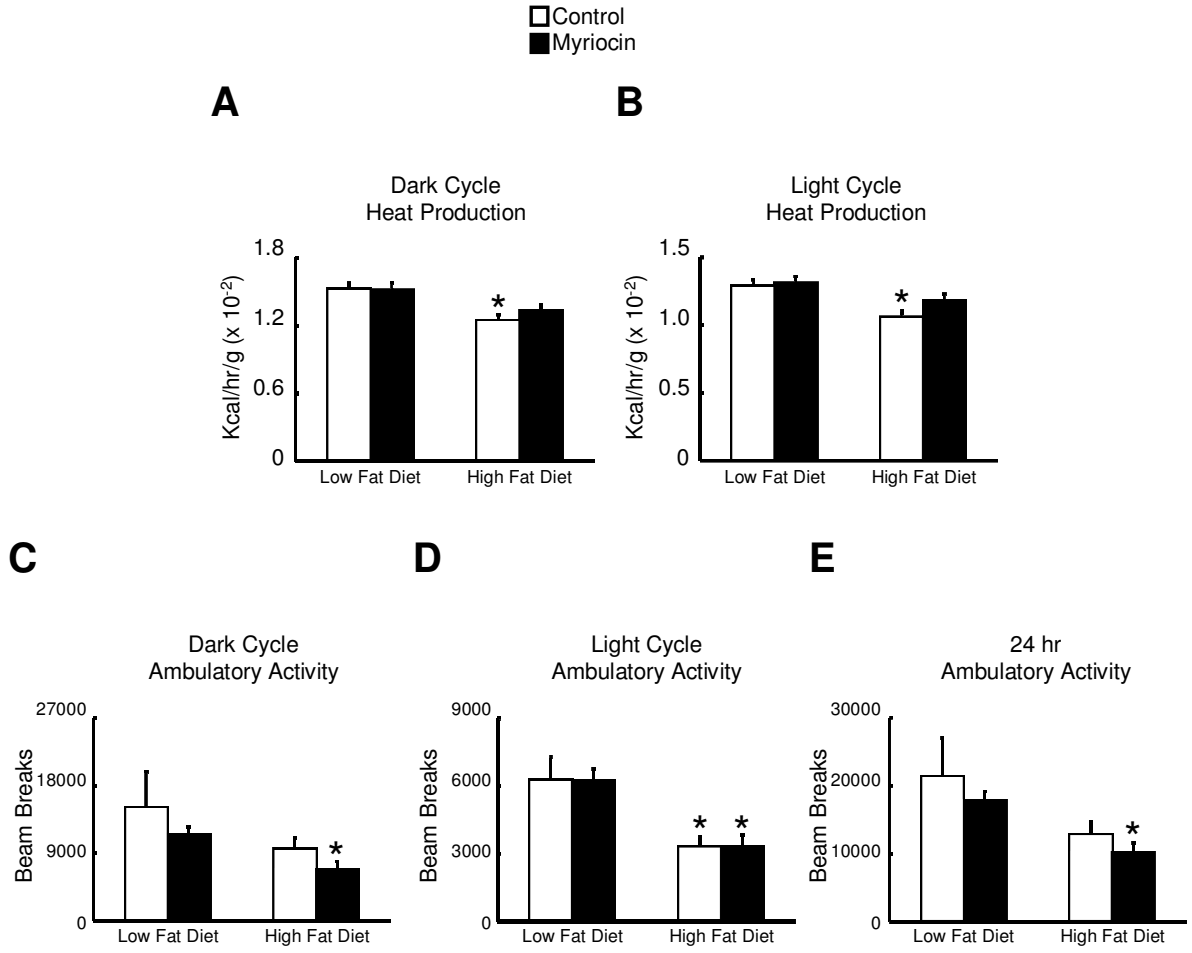

Figure 6: Citrulline levels in gastrocnemius muscle of lean and obese mice treated with either vehicle control or myriocin.
Citrulline content was measured via gas chromatography/mass spectrometry in gastrocnemius muscles from lean and obese mice treated with either vehicle control or myriocin. Values represent mean ± SE (n = 6). Differences were determined using a two-way ANOVA followed by Bonferroni post-hoc analysis. **P*<0.05, significantly different vehicle control treated counterpart.

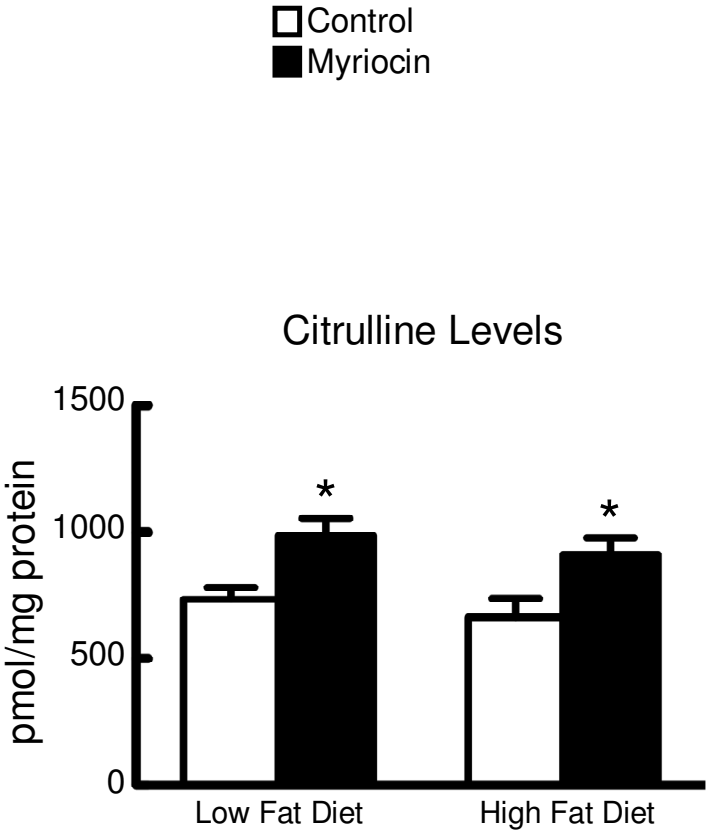

Figure 7: Hepatic lipid content and insulin signaling in lean and obese mice treated with myriocin.
A: Hepatic ceramide and *B:* TAG content from lean and obese mice treated with either vehicle control or myriocin. *C:* Insulin stimulated Akt serine 473 phosphorylation, *B:* GSK3β serine 9 phosphorylation, and *E:* AMPK threonine 172 phosphorylation in livers from obese mice treated with either vehicle control or myriocin. Values represent mean ± SE (n = 4-5). Differences were determined using a two-way ANOVA followed by Bonferroni post-hoc analysis. **P*<0.05, significantly different from low fat diet counterpart. †*P*<0.05, significantly different from control treated counterpart.

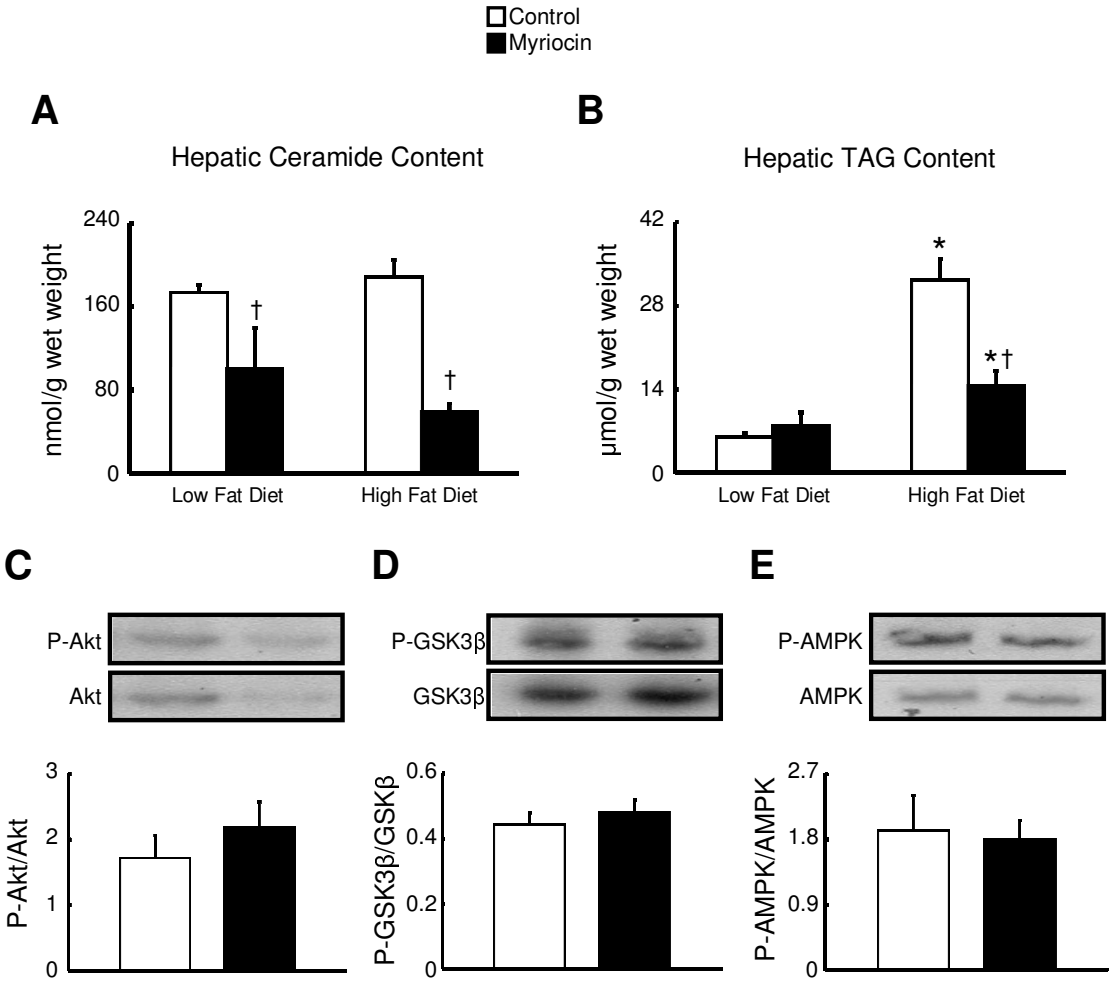

Figure 8: Gluconeogenic capacity in obese-insulin resistant mice is not altered via myriocin treatment.
A: Blood glucose levels during a pyruvate challenge in fasted, obese-insulin resistant mice treated with either vehicle control or myriocin. *B:* % change in blood glucose during the pyruvate challenge. Values represent mean ± SE (n = 4).

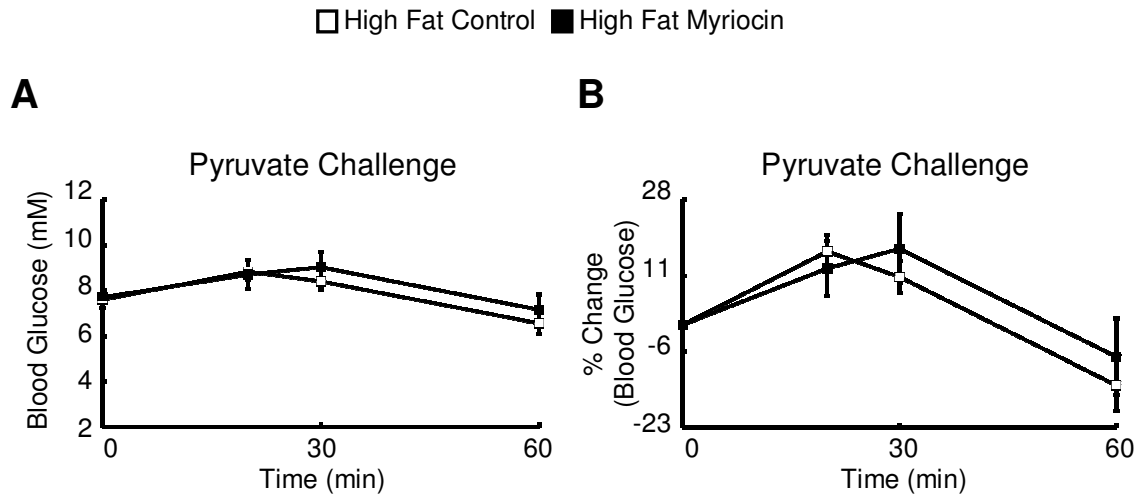

Figure 9: Expression and phosphorylation status of proteins involved in inflammation in skeletal muscle.
A: Gastrocnemius JNK phosphorylation at threonine 183, and *B:* p38 MAPK phosphorylation at threonine 180 in lean and obese mice treated with either vehicle control or myriocin. Values represent mean ± SE (n = 5-7).